Atmos. Meas. Tech. Discuss., https://doi.org/10.5194/amt-2018-299
Manuscript under review for journal Atmos. Meas. Tech.
Discussion started: 12 October 2018

Atmospheric Measurement Techniques Discussions

Development of an online-coupled MARGA upgrade for the two-hourly quantification of low-molecular weight organic acids in the gas and particle-phase

Bastian Stieger[1], Gerald Spindler[1], Dominik van Pinxteren[1], Achim Grüner[1], Markus Wallasch[2], Hartmut Herrmann[1,*]

[1]Atmospheric Chemistry Department (ACD), Leibniz Institute for Tropospheric Research (TROPOS), Permoserstraße 15, 04318 Leipzig, Germany
[2]German Federal Environment Agency, Wörlitzer Platz 1, 06844 Dessau-Roßlau, Germany

Correspondence to: Hartmut Herrmann (herrmann@tropos.de)

Abstract. A method is presented to quantify the low-molecular weight organic acids formic, acetic, propionic, butyric, pyruvic, glycolic, oxalic, malonic, succinic, malic, glutaric, and methanesulfonic acid in the atmospheric gas and particle-phase in a two-hourly time resolution, based on a combination of the Monitor for AeRosols and Gases in ambient Air (MARGA) and an additional ion chromatography (IC) instrument. A proper separation of the organic target acids was initially tackled by a laboratory IC optimization study, testing different separation columns, eluent compositions and eluent flow rates both for isocratic and for gradient elution. Satisfactory resolution of all compounds was achieved using a gradient system with two coupled anion-exchange separation columns. Online pre-concentration with an enrichment factor of approximately 400 was achieved by solid-phase extraction consisting of a methacrylate polymer based sorbent with quaternary ammonium groups. The limits of detection of the method range between 7.1 ng m^{-3} for methanesulfonate and 150.3 ng m^{-3} for pyruvate. Precisions are below 1.0 %, except for glycolate (2.9 %) and succinate (1.0 %). Comparisons of inorganic anions measured at the TROPOS research site in Melpitz, Germany, by the original MARGA and the additional organic acid IC systems are in agreement with each other (R^2 = 0.95 - 0.99). Organic acid concentrations from May 2017 as an example period are presented. Monocarboxylic acids were dominant in the gas-phase with mean concentrations of 553 ng m^{-3} for acetic acid, followed by formic (286 ng m^{-3}), pyruvic acid (182 ng m^{-3}), propionic (179 ng m^{-3}), butyric (98 ng m^{-3}) and glycolic (71 ng m^{-3}). Particulate glycolate, oxalate and methanesulfonate were quantified with mean concentrations of 63 ng m^{-3}, 74 ng m^{-3} and 35 ng m^{-3}, respectively. Elevated concentrations in the late afternoon of gas-phase formic acid and particulate oxalate indicate a photochemical formation.

1 Introduction

Low-molecular weight organic acids were measured in the gas (Lee et al., 2009;Bao et al., 2012) and particle-phase (Boreddy et al., 2017;Miyazaki et al., 2014;van Pinxteren et al., 2014) as well as in precipitation and cloud water (Sun et al., 2016;van

Pinxteren et al., 2005). Next to known primary anthropogenic (Bock et al., 2017;Kawamura and Kaplan, 1987;Legrand et al., 2007) and biogenic sources (Falkovich et al., 2005;Stavrakou et al., 2012), organic acids are formed secondary by atmospheric oxidation processes (Lim et al., 2005;Tilgner and Herrmann, 2010;Hoffmann et al., 2016). However, there are still unknown sources of these short-chained compounds (Millet et al., 2015;Stavrakou et al., 2012).

Because of their hygroscopicity (Kawamura and Bikkina, 2016), the organic acids contribute to the acidity of precipitation, dew, fog and clouds (Lee et al., 2009;van Pinxteren et al., 2016). Atmospheric transport processes also lead to dry and wet deposition in remote areas, where they can have a sensitive influence on the ecosystem (Friedman et al., 2017;Himanen et al., 2012;Sabbioni et al., 2003).

Owing to the low concentrations and the high diversity of organic acids compared to inorganic compounds, a highly resolved and near-real-time quantification of organic acids is challenging. Studies on organic compounds in particulate matter (PM) were performed with filter measurements followed by off-line analysis with ion chromatography (IC) (Röhrl and Lammel, 2002;Granby et al., 1997;Legrand et al., 2007), gas chromatography coupled with mass spectroscopy (GC/MS) (Mochizuki et al., 2018;Miyazaki et al., 2014;Kawamura et al., 2012), capillary electrophoresis (CE) (Müller et al., 2005;van Pinxteren et al., 2014;van Pinxteren et al., 2009) or Raman spectroscopy (Kuo et al., 2011).

Gas-phase compounds were sampled for a few hours and analyzed off-line with coated filters and GC/MS (Limbeck et al., 2005), denuder and GC/MS (Bao et al., 2012), denuder and IC (Dawson et al., 1980), as well as a mist chamber and IC (Preunkert et al., 2007;Schultz Tokos et al., 1992), respectively.

Due to the long sampling time of filter and wet sampling techniques followed by laboratory analyses, these methods did not allow for a near-real-time quantification and the laboratory effort is huge. Additionally, off-line filter analysis involves the risk of possible evaporation artifacts of volatile particulate compounds from the filter or the adsorption of gaseous compounds (Stieger et al., 2018) and Boring et al. (2002) mentioned the difficulty of sampling very small particles by impaction techniques. Over the last few years, new instruments have allowed online measurements with increased time resolution. Zander et al. (2010) and Pommier et al. (2016) quantified the vertical column of gaseous formic acid with ground-based Fourier transform infrared spectroscopy (FTIR). However, the focus of the present work is on the ground-based detection of the carboxylic acids because of possible influences on the lower troposphere.

Gas-phase concentrations on the ground were monitored with a Chemical Ionisation Mass Spectrometer (CIMS) (Veres et al., 2011;Liu et al., 2012;Crisp et al., 2014). This instrument also enabled airborne measurements of formic acid (Jones et al., 2014). Recently, Nah et al. (2018) assessed the use of sulfur hexafluoride (SF_6^-) anions as CIMS reagent ions as it is more sensitive for the detection of oxalic, propionic and glycolic acid. Requirements for MS analyses were already listed by Boring et al. (2002). The costs, the bulk of data and the necessity of an experienced operator limit the application for longer measurement periods. The lack of particulate data especially disqualifies the CIMS for the planned measurements.

As all organic acids are ionic, an application of the IC for the analysis is obvious. Boring et al. (2002) first described an instrument based on an IC system. The separation of the gas and particle-phase was performed by the application of a parallel plate denuder and a particle collection system consisting of glass fiber filter. The filters were washed online with deionized

water and the dissolved anions from the gas and particle-phase, including formic, acetic and oxalic acid, were analyzed. The resulting time resolution of their example measurement period was approximately 30 minutes. A disadvantage in this study was the necessary exchange of the inserted glass fiber filter every 12 hours. Fisseha et al. (2006) published results of formic, acetic, propionic and oxalic acid in Zurich, Switzerland, for three months in different seasons. These authors used a flattened denuder and an aerosol chamber under supersaturated conditions to quantify formate, acetate, propionate and oxalate in the gas and particle-phase. A detection of other dicarboxylic acids (DCA) was not possible due to co-elution with the carbonate peak and atmospheric concentrations of other monocarboxylic acids (MCA) were mostly below the detection limit of the method. Lee et al. (2009) and Ku et al. (2010) sampled only gaseous compounds with a parallel plate denuder. While the first group analyzed C1-C3 MCA within an hourly time resolution, the second group concentrated on the quantification of acetic acid every ten minutes. Recently, Zhou et al. (2015) observed gaseous and particulate oxalate in their MARGA (Monitor for AeRosols and Gases in ambient Air) measurements in Hong Kong for one year. Therefore, a pre-concentration column was installed instead of the injection loop, but the analysis of more carboxylic acids (CA) is limited by the short separation column and, thus, separation efficiency.

To the author's knowledge, online instruments properly quantifying a variety of low-molecular weight organic acids (formic, acetic, propionic, butyric, glycolic, pyruvic, oxalic, malonic, succinic, malic, glutaric, and methanesulfonic acid) within the gas and particle-phase in a high time resolution do not exist yet. The present study describes the instrumental development of an online-coupled pre-concentration and separation system to determine organic acids in the gas and particle-phase as an extension of the MARGA. The developed setup was applied from November 2016 until October 2017 at the TROPOS research site in Melpitz. As a demonstration of successful field application, first tropospheric measurements will be presented. Data interpretation of the one-year measurement campaign with focus on the phase distribution and the investigation of primary and secondary sources will be published elsewhere.

2 Instrumentation and materials

2.1 MARGA

Water-soluble chloride (Cl^-), nitrate (NO_3^-), sulphate (SO_4^{2-}), ammonium (NH_4^+), sodium (Na^+), potassium (K^+), magnesium (Mg^{2+}) and calcium (Ca^{2+}) in particles smaller than 10 µm (PM_{10}) as well as the trace gases hydrochloric acid (HCl), nitrous acid (HONO), nitric acid (HNO_3), sulfur dioxide (SO_2) and ammonia (NH_3) are quantified hourly by the commercial MARGA 1S ADI 2080 (Metrohm-Applikon, The Netherlands) (Chen et al., 2017). Its technical principles and long-term operation at the TROPOS research site in Melpitz (Spindler et al., 2013;Spindler et al., 2004) were recently described in Stieger et al. (2018). Briefly, the separation of the gas and particle-phase is performed through the usage of a Wet Rotation Denuder (WRD) and a Steam-Jet Aerosol Collector (SJAC), respectively. Both WRD and SJAC are continuously filled with an absorption solution. For one hour, syringe pumps sample 25 ml of the liquid solutions of the WRD and SJAC. Within the next hour, approximately 7 ml of each solution are transported to two ion chromatography systems to quantify the inorganic anions and

cations in both phases. The remaining sample solution is directly discarded. A continuous calibration with an internal standard (lithium bromide) is applied.

2.2 Additional IC system

In addition to the two IC systems integrated into the MARGA, an additional one (Compact-IC Flex 930, Metrohm, Switzerland) together with an autosampler (Robotic Sample Processor XL, Metrohm, Switzerland) is used for the determination of organic acids. The setup of the complete system is shown in Fig. 1. Therein, the different compounds that will be explained in the following are tagged. Comparable IC systems as for example from Thermo Scientific were considered as possible alternatives but the liquid handling via the autosampler involved problems. Especially the liquid flows from the MARGA to the necessary autosampler and the capacity of the autosampler limited the use of other IC systems.

An autosampler with two working stations (a) and (b) has a sample plate with 120 slots for 11 ml vials with perforated plugs (polypropylene; Metrohm, Switzerland). The slots are arranged in two circles. Additionally, one working station is equipped with inner and outer sample needles (a) so that the WRD and SJAC solutions can be pumped into the respective vial simultaneously. After storage, the filled vials go to the second working station consisting of a swing head with a further sample needle (b). To avoid contamination, this sample needle is cleaned in a washing station with ultrapure water after each suction. A commercial syringe pump (DOSINO 800, Metrohm, Switzerland; c) transports 10 ml of one sample from the autosampler via a 6-way injection valve within the Compact-IC (d) to a sample loop (e) with a velocity of 2 ml min^{-1}. A graphical explanation of the different modes of the 6-way-valve is in the supplement (Fig. S1). Afterwards, the injection valve switches to the fill mode and the DOSINO 800 transfers the complete sample volume into a pre-concentration column (Metrosep A PCC 2 VHC, Metrohm, Switzerland) consisting of a spherical methacrylate polymer with quaternary ammonium groups in the Compact-IC. In the injection mode, the degassed eluent consisting of 7 mM sodium carbonate (Na_2CO_3) / 0.75 mM sodium hydroxide (NaOH) desorbs the trapped ionic compounds from the pre-concentration column with a flow of 0.8 ml min^{-1} while the sample path is rinsed with ultrapure water. The anion-exchange separation column (Metrosep A Supp 16 250 mm, Metrohm, Switzerland) is stored in a column oven. Before the ionic signals are measured with a conductivity detector, the background conductivity of the anion eluent is chemically suppressed using 100 mM sulfuric acid (H_2SO_4) and 20 mM oxalic acid.

For gradient applications, a second DOSINO 800 (f) was combined with the Compact-IC. With an identical flow rate, a defined amount of a higher concentrated eluent was added to the eluent flow in front of the eluent degasser. A trap column (Metrosep A Trap 1 100/4.0) cleans and ensures a complete mixing of both eluent solutions before the eluent is injected into the pre-concentration column. For the combination of MARGA and Compact-IC, an external 6-way-valve (Metrohm, Switzerland) is required (g). The complete setup and the time program for the gradient system is controlled by the Metrohm MagIC Net software (Metrohm, Switzerland).

Atmos. Meas. Tech. Discuss., https://doi.org/10.5194/amt-2018-299
Manuscript under review for journal Atmos. Meas. Tech.
Discussion started: 12 October 2018

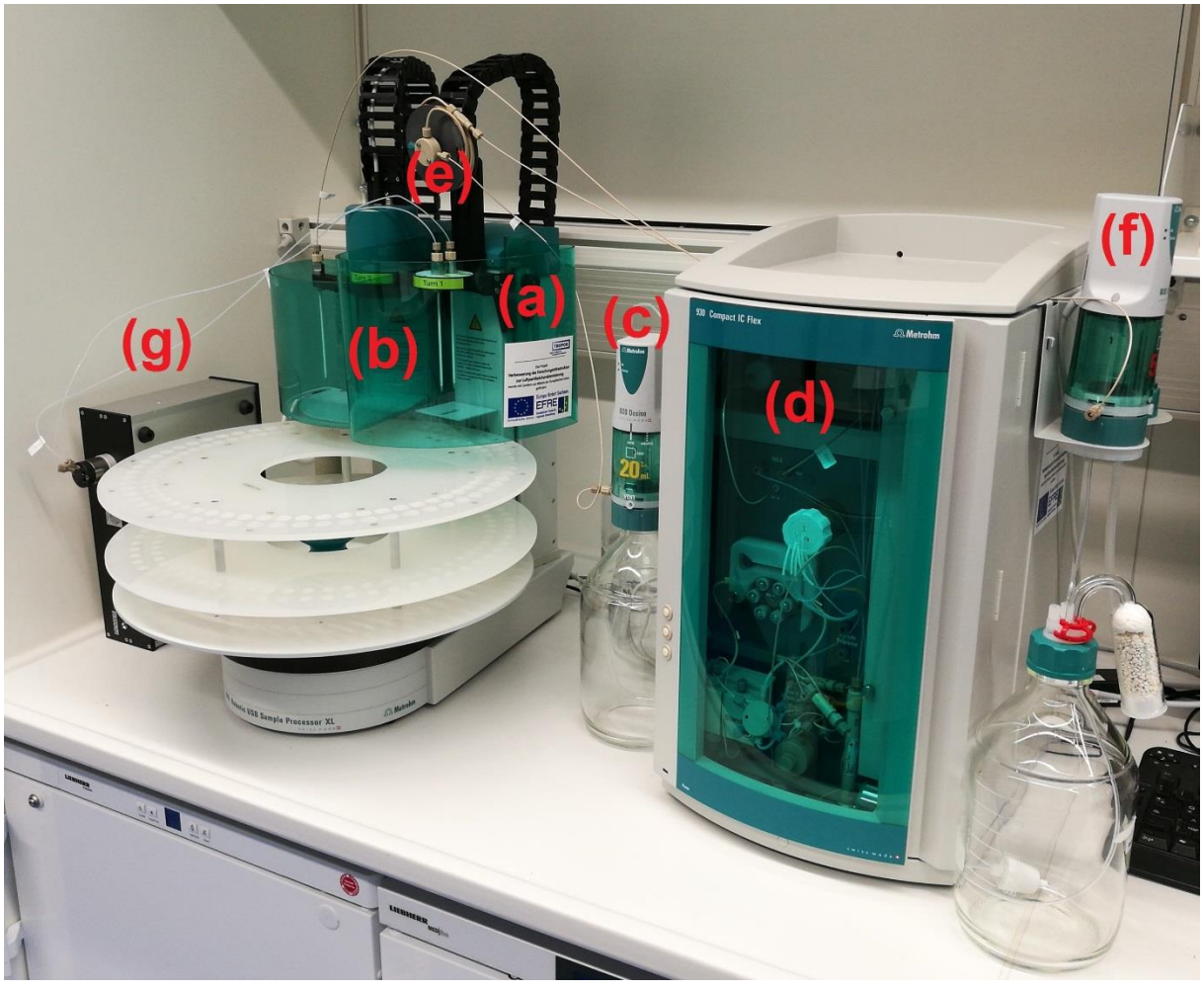

Figure 1. Setup of the IC-system with (a) the first working station and (b) the second working station of the autosampler, (c) the DOSINO 800 for the sample transportation, (d) the Compact-IC, (e) the 10 ml sample loop, (f) the DOSINO 800 for the gradient system and (g) an external 6-way-valve for the combination of MARGA and the IC-system.

The Compact-IC is manually calibrated with three standard solutions twice a week, when the vials of the autosampler are replaced. The standard solutions are prepared in 50 ml flasks, stored in the refrigerator and renewed every two weeks. The concentrations of each inorganic and organic ion are given in Table 1.

Atmos. Meas. Tech. Discuss., https://doi.org/10.5194/amt-2018-299
Manuscript under review for journal Atmos. Meas. Tech.
Discussion started: 12 October 2018

Atmospheric Measurement Techniques Discussions

Table 1. Aqueous standard solution concentrations used for the calibration of the Compact-IC.

Ions	Standard 1 / µg l^{-1}	Standard 2 / µg l^{-1}	Standard 3 / µg l^{-1}
F^-	1	10	30
Cl^-	5	50	150
NO_2^-	5	50	150
Br^-	1	10	30
NO_3^-	10	100	300
SO_4^{2-}	5	50	150
Formate	5	50	150
Acetate	5	50	150
Propionate	3	10	25
Butyrate	3	10	25
Pyruvate	3	10	25
Glycolate	3	10	25
Oxalate	3	10	25
Malonate	3	10	25
Succinate	3	10	25
Malate	3	10	25
Methanesulfonate	3	10	25

2.3 Materials

Hydrogen peroxide (H_2O_2, 30 %, Fluka) is used for the preparation of the MARGA absorption and cleaning solution. The MARGA anion and cation eluents are aqueous solutions of sodium carbonate monohydrate (99.5 %, Sigma Aldrich) and sodium bicarbonate (99.7 %, Sigma Aldrich) as well as 2 M nitric acid solution (Fluka), respectively. The MARGA internal standard and the suppressor regenerant solution are prepared with lithium bromide (99 %, Fluka) and with phosphoric acid (85 %, Fluka), respectively. For the Compact-IC eluent, sodium carbonate (Na_2CO_3) (99.5 %, Sigma Aldrich) and sodium hydroxide (NaOH) solution (50-52 %, Fluka) is dissolved. Sulfuric acid (98 %, ChemSolute) and oxalic acid (99 %, Sigma Aldrich) are mixed for the suppressor regenerant solution. The following chemicals are used for peak identification and calibration: fluoride (F^-), chloride, nitrite (NO_2^-), bromide (Br^-), nitrate, sulphate, formate, acetate, oxalate, methanesulfonate standards for IC (all 1000 mg l^{-1}, Fluka), propionic acid (99.5 %, Fluka), butyric acid (99 %, Aldrich), pyruvic acid (98 %, Aldrich), glycolic acid (99 %, Fluka), malonic acid (99 %, Fluka), succinic acid (99.5 %, Fluka), malic acid (99 %, Fluka) and glutaric acid (98 %, Fluka). All chemicals are dissolved in ultrapure water (18.2 MΩcm).

Atmos. Meas. Tech. Discuss., https://doi.org/10.5194/amt-2018-299
Manuscript under review for journal Atmos. Meas. Tech.
Discussion started: 12 October 2018

Atmospheric Measurement Techniques Discussions

3 Results and discussion

3.1 Development of the IC separation

The IC separation was developed in laboratory studies to ensure the best separation efficiency of the target compounds formate, acetate, glycolate, pyruvate, oxalate, malonate, succinate, malate, and glutarate. The further organic anions propionate, butyrate and methanesulfonate were later identified in the first field applications and then included into the standard solution. Due to their expected low concentrations, it was considered important to pre-concentrate the ions online within the aqueous MARGA sample streams from both WRD and SJAC. Therefore, a pre-concentration column was applied from the beginning of the optimization studies, as described above. An enrichment factor of 400 was achieved by the comparison of the peak areas of standard solutions applying a 20 µl injection loop and the pre-concentration column.

First analyses were performed with an isocratic system and the separation column Metrosep A Supp 16 250 mm, and the resulting chromatogram is shown in Fig. 2, based on aqueous standards with concentrations of 10 µg l^{-1} (Cl^-, NO_3^-, SO_4^{2-}), 5 µg l^{-1} (NO_2^-) and 1 µg l^{-1} (F^-, Br^-, all organic acids). The standards were loaded with a volume of 10 ml on the pre-concentration column and then desorbed into the separation column as described above. Regarding the MARGA system, these liquid concentrations would correspond to the mass concentrations of 250 ng m^{-3}, 125 ng m^{-3} and 25 ng m^{-3}, respectively. The chosen organic acid concentrations were in agreement with impactor measurements sampled in Melpitz (van Pinxteren et al., 2014). However, there was no baseline-separation of acetate and Cl^- and the concentrations of the inorganic compounds can exceed 10 µg m^{-3}, resulting in wider peaks and co-elution. This behaviour was observed for SO_4^{2-} and oxalate as well as for the first peaks between F^- and Cl^- (Fig. S2).

Since, at this stage, a satisfying separation was not achieved, other columns were additionally tested within the isocratic setup. An anion-exchange column named Shodex IC SI-50 4E (Showa Denko Europe GmbH, Germany) was included with an eluent of 3.2 mM Na_2CO_3 and 1 mM $NaHCO_3$ and an operating temperature of 30 °C. The resulting chromatogram is shown in Fig. 3a. As can be seen, almost all CAs co-eluted in two distinct peaks (peaks A and B in Fig. 3a). The MCAs formate, acetate, glycolate and pyruvate could not be separated as well as SO_4^{2-} with the DCAs malonate, succinate, malate and glutarate. As a result, this column was discarded. A Metrosep A Supp 7 250 mm (Metrohm, Switzerland) was tested with an eluent consisting of 3.2 mM Na_2CO_3 at 45 °C. The target MCAs in the chromatogram in Fig. 3b eluted close together between seven and nine minutes and a baseline-separation was not achieved. Regarding the low standard concentrations, the separation can be expected to worsen for high concentrations with this anion-exchange column. The advantage of the last two columns was the excellent separation of oxalate. However, as the aim of this work was the detection of all the target organic acids and the initial Metrosep A Supp 16 provided a good separation of all target compounds with no co-elution, this column was chosen for further improvements of the separation.

Possible improvements were investigated by changing the eluent flow and the eluent composition, which are summarized in Table 2. The flow was increased to 0.9 and 1.0 ml min^{-1} and decreased to 0.7 and 0.6 ml min^{-1}. However, only a shift of the retention times was observed that shortened or extended the analysis time, respectively. Afterwards, the eluent concentrations

Atmos. Meas. Tech. Discuss., https://doi.org/10.5194/amt-2018-299
Manuscript under review for journal Atmos. Meas. Tech.
Discussion started: 12 October 2018

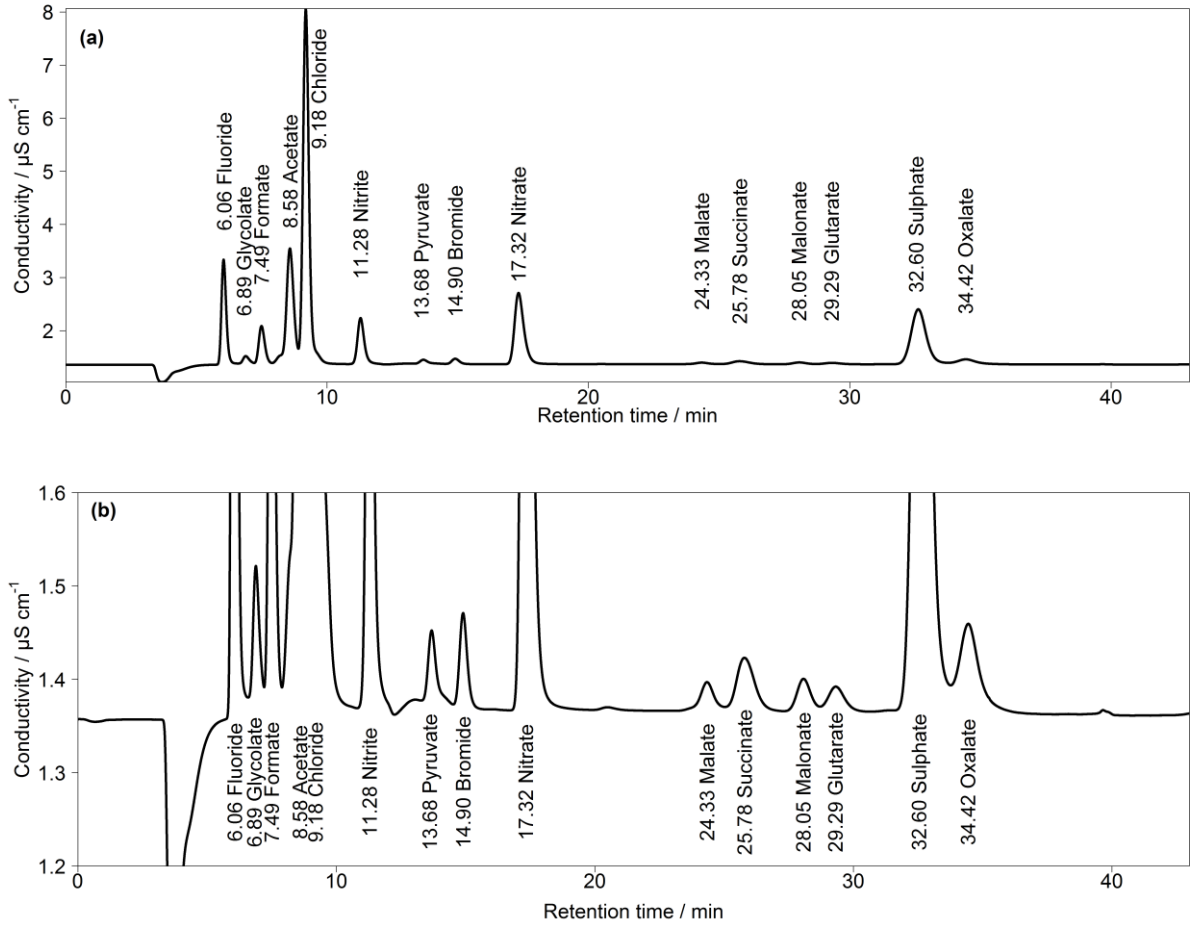

Figure 2. (a) First chromatogram of a standard solution with aqueous concentrations of 10 µg l^{-1} for Cl^-, NO_3^-, SO_4^{2-}, 5 µg l^{-1} for NO_2^- and 1 µg l^{-1} for F^-, Br^- as well as all organic acids. Numbers in front of the ion names are the retention times. T = 65 °C and eluent flow of 0.8 ml min^{-1}. (b) Zoom in of (a).

were varied. An impact of NaOH in the eluent was not observed. The retention time shift was negligible and the separation was not affected. Detectable improvements were found for lower Na_2CO_3 concentrations between F^- and Cl^-. The best separation for the MCAs was found for 6 mM Na_2CO_3. Here, glycolate and formate were baseline separated and the separation of acetate and Cl^- was improved. However, the small peaks of the DCA were broadened, which could have a negative influence on the peak detection, especially for oxalate that is near the tailing of SO_4^{2-}. An eluent composition of 8 mM Na_2CO_3 led to sharper DCA peaks, but worsened the MCA separation.

Atmos. Meas. Tech. Discuss., https://doi.org/10.5194/amt-2018-299
Manuscript under review for journal Atmos. Meas. Tech.
Discussion started: 12 October 2018

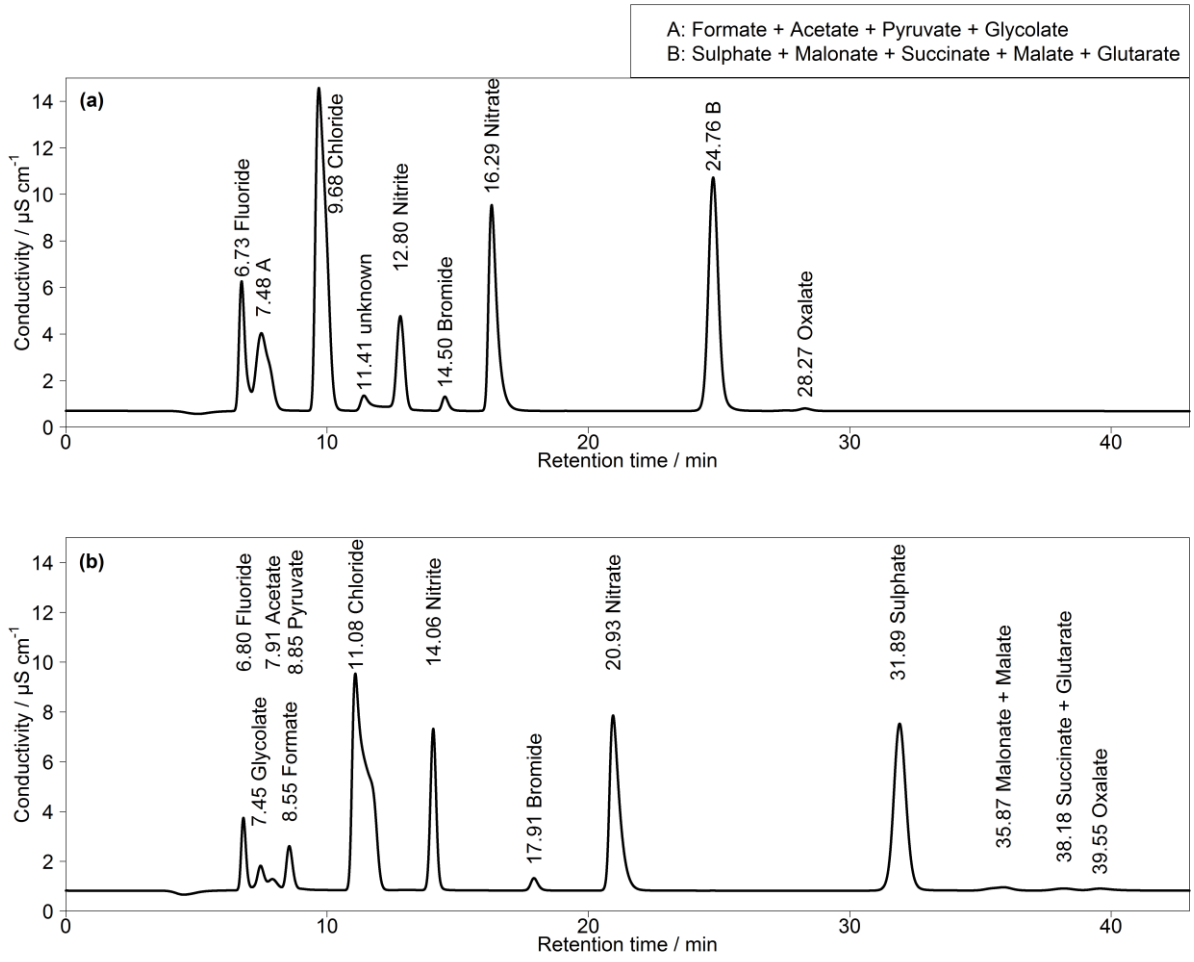

Figure 3. (a) Isocratic chromatogram for Shodex IC SI-50 4E with a standard solution of 50 µg l^{-1} for Cl^-, NO_3^-, SO_4^{2-}, 25 µg l^{-1} for NO_2^- and 5 µg l^{-1} for F^-, Br^- as well as 2 µg l^{-1} for all organic acids (T = 30 °C, eluent flow = 0.7 ml min^{-1}). (b) Isocratic chromatogram for Metrosep A Supp 7 with a standard solution of 50 µg l^{-1} for Cl^-, NO_3^-, SO_4^{2-}, 25 µg l^{-1} for NO_2^- and 5 µg l^{-1} for F^-, Br^- as well as 3 µg l^{-1} for all organic acids (T = 45 °C, eluent flow = 0.8 ml min^{-1}). Numbers in front of the ion names indicate the retention times in min.

To combine the advantages of the different eluent compositions, a gradient system was applied. Two differently concentrated eluents were prepared. Within the Compact-IC, a highly concentrated eluent B (20 mM Na_2CO_3) was mixed with a lower concentration eluent A (0.5 mM Na_2CO_3). An example of the resulting chromatogram with the respective time program is shown in Fig. 4. In this example, the fraction of eluent B was increased to 50% shortly before the beginning of the analysis to shorten the analysis time before of the F^- peak. At retention time t = 5 min the eluent B was set to 0 %, which enabled a baseline-separation of the MCAs. At t = 15 min, eluent B was rapidly increased to 50 % to accelerate the analysis and, additionally, to obtain sharper peaks of SO_4^{2-} and the DCAs. For succeeding analyses, it was important to decrease eluent B to

Atmos. Meas. Tech. Discuss., https://doi.org/10.5194/amt-2018-299
Manuscript under review for journal Atmos. Meas. Tech.
Discussion started: 12 October 2018

Atmospheric Measurement Techniques Discussions

Table 2. Overview of varied flows and eluent compositions in the isocratic system using column Metrosep A Supp 16 250 mm with their effects on separation and reference to the corresponding figures in the supplement.

	Flow	Eluent composition	Effect on separation	supplement
1	0.8 ml min^{-1}	7 mM Na_2CO_3 / 0.75 mM NaOH	reference	
2	0.6 ml min^{-1}	7 mM Na_2CO_3 / 0.75 mM NaOH	longer analysis time, shift of retentions times	S3
3	0.7 ml min^{-1}	7 mM Na_2CO_3 / 0.75 mM NaOH	longer analysis time, shift of retentions times	S4
4	0.9 ml min^{-1}	7 mM Na_2CO_3 / 0.75 mM NaOH	shorter analysis time, shift of retentions times	S5
5	1.0 ml min^{-1}	7 mM Na_2CO_3 / 0.75 mM NaOH	shorter analysis time, shift of retentions times	S6
6	0.8 ml min^{-1}	6 mM Na_2CO_3 / 0.75 mM NaOH	improved baseline-separation for MCA, broad DCAs	S7
7	0.8 ml min^{-1}	6.5 mM Na_2CO_3 / 0.75 mM NaOH	improved baseline-separation for MCA, broad DCAs	S8
8	0.8 ml min^{-1}	7.5 mM Na_2CO_3 / 0.75 mM NaOH	sharper DCA peaks, weaker MCA separation	S9
9	0.8 ml min^{-1}	8 mM Na_2CO_3 / 0.75 mM NaOH	sharper DCA peaks, weaker MCA separation	S10
10	0.8 ml min^{-1}	7 mM Na_2CO_3 / 0.65 mM NaOH	no improvements	S11
11	0.8 ml min^{-1}	7 mM Na_2CO_3 / 0.7 mM NaOH	no improvements	S12
12	0.8 ml min^{-1}	7 mM Na_2CO_3 / 0.8 mM NaOH	no improvements	S13
13	0.8 ml min^{-1}	7 mM Na_2CO_3 / 0.85 mM NaOH	no improvements	S14

0 % at t = 38 min. Otherwise, a shift of the retention times in the next analysis occurred because of a carryover of eluent B. Thus, the column was flushed with 100 % eluent A between analyses. The overall eluent profile is shown in Fig. 4a.

Atmos. Meas. Tech. Discuss., https://doi.org/10.5194/amt-2018-299
Manuscript under review for journal Atmos. Meas. Tech.
Discussion started: 12 October 2018

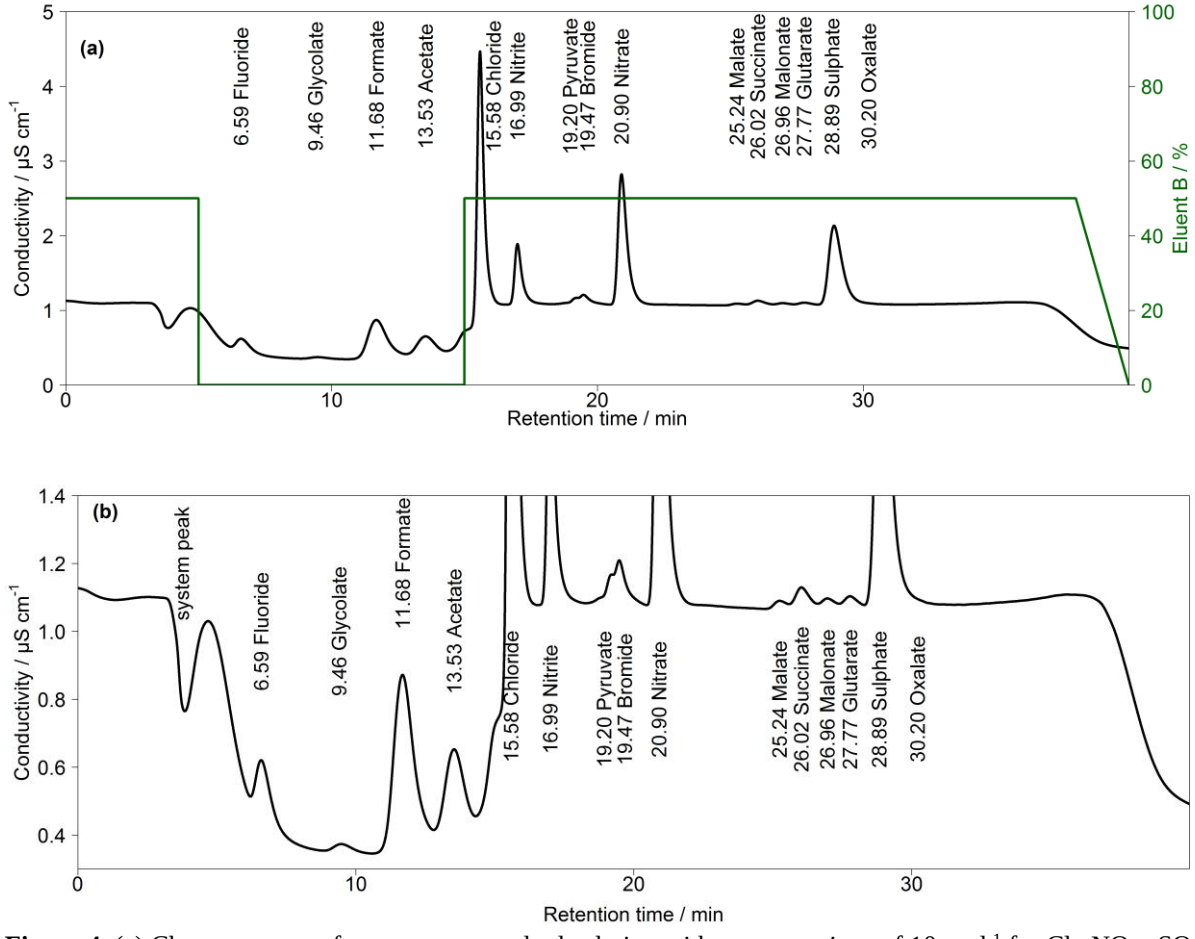

Figure 4. (a) Chromatogram of an aqueous standard solution with concentrations of 10 µg l^{-1} for Cl^-, NO_3^-, SO_4^{2-}, 5 µg l^{-1} for NO_2^- and 1 µg l^{-1} for F^-, Br^- as well as all organic acids with the gradient system. Numbers in front of the ion names indicate the retention times in min. The fraction of eluent B within the eluent mixture over time is given as green line. The eluent concentration of A is 0.5 mM Na_2CO_3 / 0.75 mM NaOH and of B is 20 mM Na_2CO_3 / 0.75 mM NaOH. T = 65 °C and eluent flow of 0.8 ml min^{-1}. (b) Zoom in of (a).

Although the MCA separation was improved by applying the described gradient, no baseline-separated pyruvate and Br^- was observed. In addition, the DCA eluted very closely and oxalate co-eluted with the tailing of the SO_4^{2-} peak.

Change the oven temperature was also considered. All measurements with the Metrosep A Supp 16 250 mm were executed with a temperature of 65 °C, which is the maximum temperature of the oven. Tests with 55 °C resulted in a shift of the retention times compared to an analysis with 65 °C, which is shown in Fig. S15. While the oxalate peak was sharper for the lower oven temperature, separation of the pyruvate and Br^-, as well as the other DCAs, was still not satisfactory.

To improve peak resolutions, the Metrosep A Supp 16 250 mm was prolonged with an additional Metrosep A Supp 16 150 mm (Metrohm, Switzerland) column. An even longer second column could not be chosen because of a system pressure limitation of 20 MPa that would otherwise be exceeded. Resulting from the increased back-pressure of the long coupled columns, it was necessary to keep the oven temperature at 65 °C, because lower temperatures would increase the system pressure above its limit. The chromatogram in Fig. 5 shows an improved separation with the prolonged column system.

The gradient profile was adjusted for this separation. First analyses were performed with the described profile of Fig. 4 but the retention times were not stable. The longer analysis time of 52.5 min and, thus, the shorter regeneration time between the analyses led to carryovers of eluent B. Therefore, other gradient profiles were tested and the best result was found starting with 100 % of eluent A. Afterwards, eluent B was slowly increased to 40 % from t = 8 min until t = 25 min. This ensured a proper separation of all MCAs. The concentration of eluent B was kept constant until t = 50 min, yielding an improved separation of DCAs as well as of SO_4^{2-} and oxalate, even for higher SO_4^{2-} concentrations. After t = 50 min, the eluent B was decreased to 0 %. The overall eluent profile is shown in Fig. 5. The small peak behind acetate was identified as lactate. This ion was only detected in standard solutions, but was not observed in ambient samples. Thus, a contamination by the used chemicals or the used glassware is likely.

The described method allowed for the proper separation of all organic target anions, which is why this system was selected and applied for real atmospheric analyses.

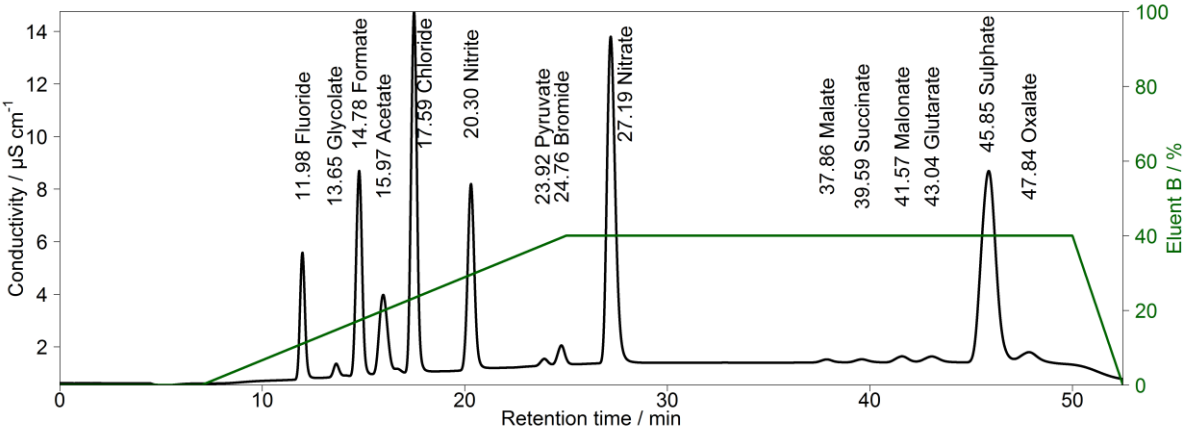

Figure 5. Chromatogram of combined Metrosep A Supp 16 250 mm and 150 mm with a gradient. The concentrations of the standard solution are 50 µg l^{-1} for Cl^-, NO_2^-, Formate and Acetate; 100 µg l^{-1} for NO_3^-, SO_4^{2-}; 10 µg l^{-1} for and 10 µg l^{-1} for F^-, Br^- as well as all organic acids with a gradient system. Numbers in front of the ion names indicate the retention times in min. The fraction of eluent B within the eluent mixture over time is given as green line. The eluent concentration of A is 0.5 mM Na_2CO_3 / 0.75 mM NaOH and of B is 20 mM Na_2CO_3 / 0.75 mM NaOH. T = 65 °C and eluent flow of 0.8 ml min^{-1}.

Atmos. Meas. Tech. Discuss., https://doi.org/10.5194/amt-2018-299
Manuscript under review for journal Atmos. Meas. Tech.
Discussion started: 12 October 2018

Atmospheric Measurement Techniques Discussions

3.2 Limits of detection and precision

The limit of detection (LOD) of each ion was determined following the norms DIN 32645 (DIN 32645, 2008) for linear calibration functions as well as DIN 8466-2 (DIN ISO 8466-2, 2004) for non-linear second-order calibration functions published by the German Institute for Standardization (DIN). Both norms are explained in the following.

For the linear calibration function ($y = a + bx$), the slope b and the intercept a can be calculated as follows (DIN 32645, 2008):

$$Q_{xx} = \sum_{i=1}^{n} x_i^2 - \frac{(\sum_{i=1}^{n} x_i)^2}{n} \quad (1)$$

$$Q_{yy} = \sum_{i=1}^{n} y_i^2 - \frac{(\sum_{i=1}^{n} y_i)^2}{n} \quad (2)$$

$$Q_{xy} = \sum_{i=1}^{n} (x_i y_i) - \frac{\sum_{i=1}^{n} x_i \sum_{i=1}^{n} y_i}{n} \quad (3)$$

$$b = \frac{Q_{xy}}{Q_{xx}} \quad (4)$$

$$a = \bar{y} - b\bar{x} \quad (5)$$

where Q_{xx}, Q_{yy} and Q_{xy} are the square sums, $\bar{x}$ and $\bar{y}$ the means and n the number of calibration points.

The calibration of a non-linear second-order function ($y = a + bx + cx^2$) was calculated considering DIN ISO 8466-2 (2004). Simultaneous to the Eq. (1) to (3), the following quadratic sums were added:

$$Q_{x^3} = \sum_{i=1}^{n} x_i^3 - \sum_{i=1}^{n} x_i \frac{\sum_{i=1}^{n} x_i^2}{n} \quad (6)$$

$$Q_{x^4} = \sum_{i=1}^{n} x_i^4 - \frac{(\sum_{i=1}^{n} x_i^2)^2}{n} \quad (7)$$

Atmos. Meas. Tech. Discuss., https://doi.org/10.5194/amt-2018-299
Manuscript under review for journal Atmos. Meas. Tech.
Discussion started: 12 October 2018

Atmospheric Measurement Techniques Discussions

$$Q_{x^2y} = \sum_{i=1}^{n}(x_i^2 y_i) - \sum_{i=1}^{n} y_i \frac{\sum_{i=1}^{n} x_i^2}{n} \tag{8}$$

The intercept a and the coefficients b and c were calculated as follows:

$$c = \frac{Q_{xy}Q_{x^3} - Q_{x^2y}Q_{xx}}{Q_{x^3}^2 - Q_{xx}Q_{x^4}} \tag{9}$$

$$b = \frac{Q_{xy} - cQ_{x^3}}{Q_{xx}} \tag{10}$$

$$a = \bar{y} - b\bar{x} - c\frac{\sum_{i=1}^{n} x_i^2}{n} \tag{11}$$

The residual standard deviation for the linear $s_{y,l}$ and the non-linear case $s_{y,nl}$ are:

$$s_{y,l} = \sqrt{\frac{\sum_{i=1}^{n}[y_i - (bx_i + a)]^2}{n-2}} = \sqrt{\frac{Q_{yy} - \frac{Q_{xy}^2}{Q_{xx}}}{n-2}} \tag{12}$$

$$s_{y,nl} = \sqrt{\frac{\sum_{i=1}^{n}(y_i - \hat{y}_i)^2}{n-3}} \tag{13}$$

To test each ion's linearity, the difference of the variances DS^2 was calculated with (Funk et al., 2005)

$$DS^2 = (n-2)s_{y,l}^2 - (n-3)s_{y,nl}^2 \tag{14}$$

with the degree of freedom of $f = 1$. For a F-Test, the test value TV was determined:

$$TV = \frac{DS^2}{s_{y,nl}^2} \tag{15}$$

Atmos. Meas. Tech. Discuss., https://doi.org/10.5194/amt-2018-299
Manuscript under review for journal Atmos. Meas. Tech.
Discussion started: 12 October 2018

Atmospheric Measurement Techniques Discussions

This test value was compared with a F-Test table ($f_1 = 1$, $f_2 = n - 3$, $P = 99$ %). If $TV \leq F$, the calibration function is linear. For the other cases, the calibration function is a non-linear second-order function. In case of the present work is $F = 11.26$. The resulting TV values for each ion are summarized in Table S1. Depending on the result of the linearity test, linear or quadratic calibration functions were fitted. As examples for a linear and a quadratic fit, the calibration functions of NO_3^- and pyruvate are respectively displayed in Fig. 6. Other calibration functions are given in the supplement (Fig. S16).

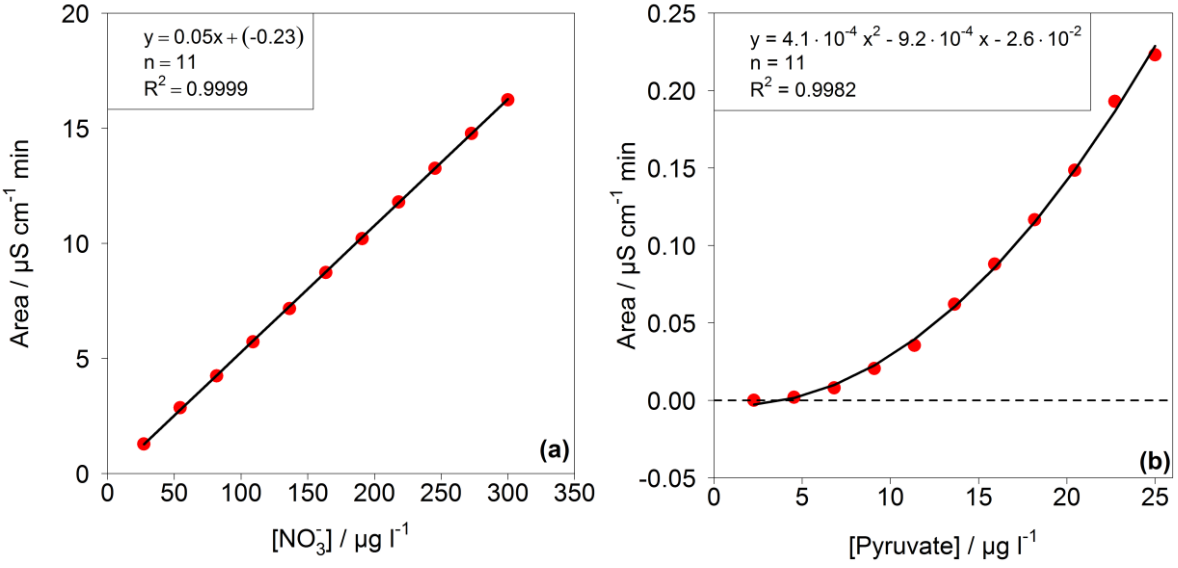

Figure 6. (a) Linear (NO_3^-) and (b) quadratic (pyruvate) calibration function.

For the linear case, the standard deviation of the method was calculated as quotient of the residual standard deviation and the slope b results in the standard deviation of the method:

$$s_{x0} = \frac{s_y}{b} \tag{16}$$

For the linear case, the upper and lower limits of the prediction interval is given by

$$y_{u,l} = (bx + a) \pm s_y t_{f,\alpha} \sqrt{\frac{1}{n} + \frac{1}{m} + \frac{(x - \bar{x})^2}{Q_{xx}}} \tag{17}$$

Atmos. Meas. Tech. Discuss., https://doi.org/10.5194/amt-2018-299
Manuscript under review for journal Atmos. Meas. Tech.
Discussion started: 12 October 2018

Atmospheric Measurement Techniques Discussions

where $t_{f,\alpha}$ is the t-value for $f = (n-2)$ degrees of freedom for a significance level $\alpha = 0.05$ and m is the number of measurements. According to DIN 32645 (2008), the LOD x_{LOD} corresponds to a critical value y_c that is equal to the one-sided upper prediction interval y_u at $x = 0$:

$$y_c = a + s_y t_{f,\alpha} \sqrt{\frac{1}{n} + \frac{1}{m} + \frac{\bar{x}^2}{Q_{xx}}} \tag{18}$$

$$y_c = b x_{LOD} + a \tag{19}$$

$$x_{LOD} = \frac{y_c - a}{b} \tag{20}$$

$$x_{LOD} = \frac{s_y t_{f,\alpha}}{b} \sqrt{\frac{1}{n} + \frac{1}{m} + \frac{\bar{x}^2}{Q_{xx}}} \tag{21}$$

$$x_{LOD} = s_{x0} t_{f,\alpha} \sqrt{\frac{1}{n} + \frac{1}{m} + \frac{\bar{x}^2}{Q_{xx}}} \tag{22}$$

For the non-linear case, the critical value y_c for second-order functions at $x = 0$ is

$$y_c = a + s_y t_{f,\alpha} \sqrt{\frac{1}{n} + \frac{1}{m} + T} \tag{23}$$

resulting in the calculation of x_{LOD}

$$x_{LOD} = -\frac{b}{2c} \pm \sqrt{\frac{b^2}{4c^2} \pm \frac{a - y_c}{c}} \tag{24}$$

$$x_{LOD} = -\frac{b}{2c} \pm \sqrt{\frac{b^2}{4c^2} \pm \frac{s_y t_{f,\alpha} \sqrt{\frac{1}{n} + \frac{1}{m} + T}}{c}} \tag{25}$$

Atmos. Meas. Tech. Discuss., https://doi.org/10.5194/amt-2018-299
Manuscript under review for journal Atmos. Meas. Tech.
Discussion started: 12 October 2018

where term T is

$$T = \frac{\bar{x}^2 Q_{x^4} + \left(\frac{\sum_{i=1}^{n} x_i^2}{n}\right)^2 Q_{xx} - 2\bar{x}\frac{\sum_{i=1}^{n} x_i^2}{n} Q_{x^3}}{Q_{x^4} Q_{xx} - Q_{x^3}^2} \quad (26)$$

and the $\pm$ in Eq. (24) and (25) is $+$ for convex and $-$ for concave calibration functions. The degree of freedom is $f = (n - 3)$. The calibration was performed through a double injection of 11 standards with evenly distributed concentrations over one order of magnitude, where the maximum concentration corresponded to standard 3 in Table 1.

The resulting linearity, LODs and precision are given in Table 3. The LODs as atmospheric concentrations varied between 4.5 ng m^{-3} for F^- and 150.3 ng m^{-3} for pyruvate and were considered sufficiently low for field application of the system. The precision of the method was calculated as the relative standard deviation (RSD) of peak areas of 11 injections of standard 3 (Table 1) over one month. The percent values can be found in Table 3. For all ions, the precision is below 3 %, indicating a good repeatability.

Atmos. Meas. Tech. Discuss., https://doi.org/10.5194/amt-2018-299
Manuscript under review for journal Atmos. Meas. Tech.
Discussion started: 12 October 2018

Table 3. Type of calibration curve, LODs and the method precision for each ion.

Ion	Cal. curve	LOD / ng m^{-3}	precision / %
F^-	quadratic	4.5	0.3
Cl^-	linear	21.3	1.9
NO_2^-	linear	23.7	0.4
Br^-	quadratic	17.0	0.2
NO_3^-	linear	41.9	0.7
SO_4^{2-}	quadratic	28.2	0.4
Methanesulfonate	quadratic	7.1	0.5
Formate	linear	52.5	0.5
Acetate	quadratic	89.6	1.0
Glycolate	quadratic	10.6	2.9
Propionate	linear	16.0	0.7
Butyrate	linear	36.5	0.5
Pyruvate	quadratic	150.3	0.1
Oxalate	linear	21.1	0.1
Malonate	linear	9.9	0.1
Malate	quadratic	46.4	0.2
Succinate	quadratic	103.6	1.0
Glutarate	quadratic	17.4	0.1

3.3 Sample handling

For the combination of the MARGA and the new IC setup, the liquid flows in the system had to be adjusted to achieve a high time resolution and to analyze the solutions as fast as possible after the sampling. As an overview, a schematic setup and a time diagram in Fig. 7 display the important steps for the CA analysis of the WRD and SJAC samples. Therein, the sampled airflow is described with green arrows. Syringe pumps within the MARGA collected the dissolved ions within the WRD (blue arrows) and SJAC (red arrows) solutions. This sampling required one hour.

In the second hour, the MARGA syringe pumps transported the solutions to the IC system within the MARGA to analyze the inorganic compounds in the gas and particle-phase, but only for 15 min each. During the remaining time, the samples were transported via an external 6-way-valve (Fig. 1 (g)) either to the autosampler or to the waste. As the vials in the autosampler had a volume of 11 ml, the 6-way-valve transferred the samples to the autosampler only for 30 minutes and the rest of the solutions were directed into the waste. In the third and fourth hour, the WRD and SJAC samples were successively pre-concentrated and analyzed.

Atmos. Meas. Tech. Discuss., https://doi.org/10.5194/amt-2018-299
Manuscript under review for journal Atmos. Meas. Tech.
Discussion started: 12 October 2018

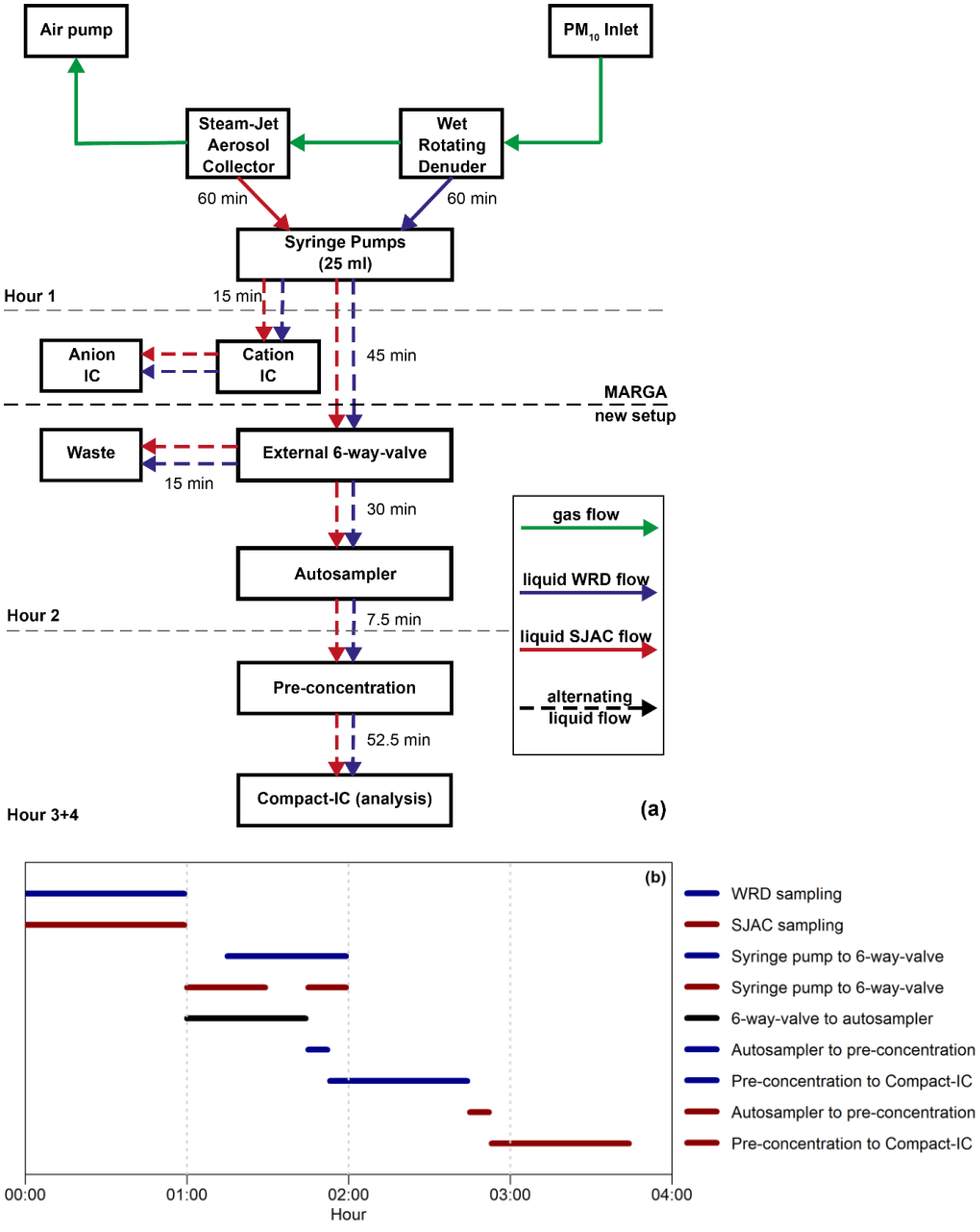

Figure 7. (a) Schematic overview of the sample handling for the complete setup (MARGA and new setup). Green arrows illustrate gas flow, while blue and red are the aqueous WRD and SJAC samples, respectively. The time on the arrows represents the flow duration. Dashed arrows stand for alternating flows. Grey dashed lines illustrate the hourly time steps, while the black bold dashed line is the border between MARGA and new IC system. (b) Time diagram of the liquid handling (blue: WRD, red: SJAC). Black is the open mode of the 6-way-valve for liquid transport from the syringe pumps to the autosampler.

To achieve a two-hourly time resolution, the aim was to pre-concentrate and analyze one sample in exactly 60 minutes. As the final Compact-IC analysis described previously needed 52.5 minutes, the transfer of analytes from the autosampler to the Compact-IC and the pre-concentration had to be performed within the remaining 7.5 minutes. Therefore, the sample flows were increased to 4 ml min^{-1}, which is the maximum for what is allowed for the pre-concentration column.

In the following, the MARGA and the Compact-IC analysis will be distinguished. Analyzed ions by the MARGA were measured by the original MARGA system, while ions from the Compact-IC were measured by the added setup.

3.4 MARGA absorption solution

The MARGA absorption solution in the denuder and SJAC contains H_2O_2 in its original setup to avoid biological contamination of the system and to oxidize absorbed SO_2 into SO_4^{2-}. However, H_2O_2 can affect the concentration of dissolved CAs through oxidation. As an example, Schöne and Herrmann (2014) described a fast degradation of pyruvate in an aqueous H_2O_2 solution and a simultaneous increase of acetate as a product. This would result in incorrect concentrations within the aqueous gas and particle-phase samples. Therefore, H_2O_2 was not added during the CA measurements and ultrapure water was used as absorption solution. With the missing oxidant, however, an underestimation of measured MARGA SO_2 occurred that required further adjustments. A MARGA software update by Metrohm-Applikon, the Netherlands, allowed integrating the sulphite peak and calculating the overall SO_2 concentration as a sum of sulphite and SO_4^{2-}. For the Compact-IC analysis, the sulphite peak was located between glutarate and SO_4^{2-} and did not interfere with the quantification of the organic acids.

Because of the missing biocide H_2O_2, the MARGA was cleaned more frequently, at least every two weeks to avoid bacterial contamination. The WRD and SJAC were rinsed with ethanol as well as ultrapure water and afterwards a system cleaning procedure was applied. Therein, the absorption solution was replaced by a 1 % H_2O_2 solution with maximal syringe pump speed for at least three hours. Before the next MARGA analysis, the complete MARGA system was rinsed for two hours with ultrapure water to remove the H_2O_2.

3.5 Intercomparison of inorganic ions

Both MARGA and Compact-IC determined the inorganic compounds in the gas and particle-phase from the same aqueous solution but used different IC methods, including a different calibration, different sample enrichments, different separation columns and different eluent compositions and profiles. For quality assurance, the inorganic ions were compared in the gas and particle-phase for the complete one-year field application of the extended MARGA system and the results are summarized numerically in Table 4 as well as graphically in Fig. S17 and S18.

The Cl^-, NO_3^- and SO_4^{2-} concentrations measured by the MARGA and the Compact-IC were in good agreement with $R^2 = 0.95$, $R^2 = 0.97$ and $R^2 = 0.99$, respectively, and slopes close to unity. It should be noted that the MARGA measured the overall SO_2 concentration because of the quantification of sulphite and SO_4^{2-}, while the Compact-IC quantified only SO_4^{2-} and not the sulphite peak. Thus, higher MARGA SO_2 concentrations were expected. An underestimation of the SO_2 concentration by the Compact-IC was indeed obvious, especially for lower concentrations. However, the overall correlation for SO_2 was found to

be good with a slope of 0.98 and an R^2 of 0.97. It is likely that the WRD absorbed gaseous atmospheric oxidants that oxidized sulphite into SO_4^{2-} in the aqueous WRD solution, even without the addition of H_2O_2 to the absorption solution, as described above. With slopes around 1.5, the regression parameters of HCl and HNO_3 are comparable with each other. The slope for the HCl comparison is a result of three MARGA outliers with concentrations higher than 4 µg m^{-3}. Without these outliers the slope decreased to 1.16 and the coefficient of determination to R^2 = 0.79. A decrease from R^2 = 0.77 to R^2 = 0.57 was observed when HNO_3 concentrations above 3 µg m^{-3} were removed. The elimination of the outliers did not result in an improvement of the slope. In the case of HNO_3 and partly of HCl, the MARGA quantified higher concentrations for the same aqueous solution. Rumsey and Walker (2016) found a quadratic response for low HNO_3 concentrations and hypothesized an overestimation of MARGA concentrations. The same was possible for HCl. In the present study, the particulate concentrations were higher and the quadratic influence is of minor importance, leading to slopes near unity.

Table 4. Orthogonal regression parameters of the comparison of inorganic compounds measured by MARGA and Compact-IC in Melpitz for one year. Scatter plots are given in Fig. S17 and S18.

Phase	Ion	Slope	Intercept	R^2	n
gas	HCl	1.50	-0.08	0.92	1358
	HONO	0.80	0.20	0.59	2713
	SO_2	0.98	0.12	0.97	2558
	HNO_3	1.51	0.00	0.76	2570
particle	Cl^-	1.11	-0.02	0.95	1768
	NO_3^-	1.02	0.20	0.99	2707
	SO_4^{2-}	0.88	0.39	0.97	2705

The HONO comparison revealed an obvious scattering (R^2 = 0.59). Possible reactions between sampling and analysis altered the HONO concentrations. Spindler et al. (2003) observed and quantified the artifact sulphate and HONO formation by reactions of dissolved NO_2 and SO_2 within the aqueous solution of the WRD. Between the MARGA and the Compact-IC analysis for the WRD samples one hour passes where such artifact formation could occur. However, the intercomparison of the more stable inorganic ions demonstrated a good comparability between MARGA and Compact-IC data.

3.6 Example application in the field

Measurements with the extended MARGA setup were performed in Melpitz for one year. Here, data from two weeks are presented to show the successful application in the field. Figure 8 displays the measured organic acids in the gas and particle-

Atmos. Meas. Tech. Discuss., https://doi.org/10.5194/amt-2018-299
Manuscript under review for journal Atmos. Meas. Tech.
Discussion started: 12 October 2018

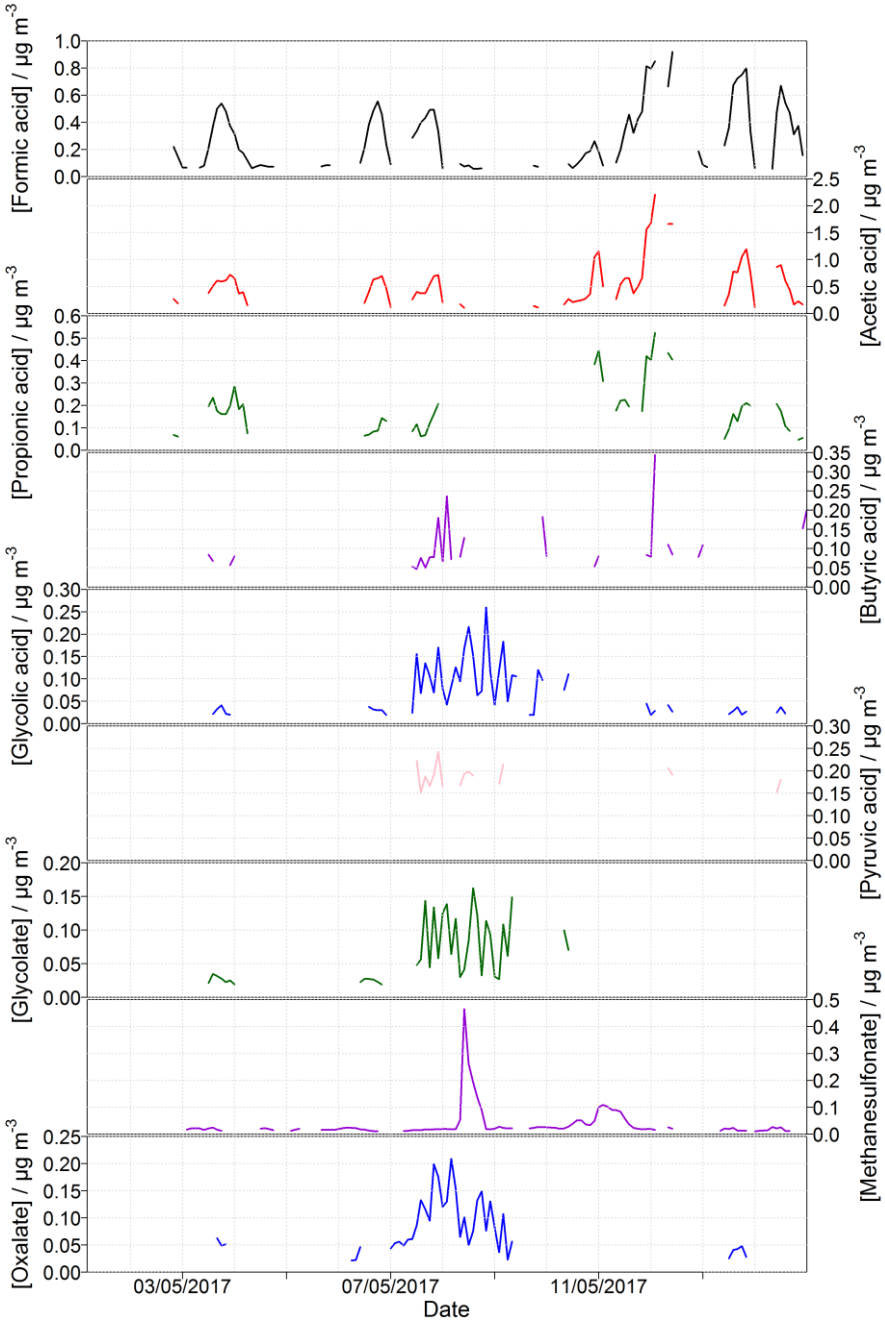

Figure 8. Measured concentrations for gaseous formic, acetic, propionic, butyric, glycolic and pyruvic acid as well as for particulate glycolate, methanesulfonate and oxalate from 1st May until 14th May 2017 for an example application.

phase from 1st May 2017 until 14th May 2017. Meteorological conditions are illustrated in Fig. S19. All MCAs were found in the gas-phase agreeing with higher vapour pressures of MCAs (Howard and Meylan, 1997). Mean (maximum) concentrations

Atmos. Meas. Tech. Discuss., https://doi.org/10.5194/amt-2018-299
Manuscript under review for journal Atmos. Meas. Tech.
Discussion started: 12 October 2018

Atmospheric Measurement Techniques Discussions

of 553 ng m^{-3} (2.2 µg m^{-3}) were achieved for acetic acid followed by formic 286 ng m^{-3} (0.9 µg m^{-3}), pyruvic 182 ng m^{-3} (0.25 µg m^{-3}), propionic 179 ng m^{-3} (0.52 µg m^{-3}), butyric 98 ng m^{-3} (0.34 µg m^{-3}) and glycolic acid 71 ng m^{-3} (0.26 µg m^{-3}). A diurnal cycle was observed for formic acid, which is illustrated in Fig. 9a. Formic acid had the lowest concentrations in the early morning and increased in the afternoon until the maxima were reached in the evening indicating a photochemical formation of these compounds. This is in agreement with previous studies (Lee et al., 2009;Millet et al., 2015;Khare et al., 1997;Nah et al., 2018).

Corresponding ions in the particle-phase were only measured for glycolate. Glycolate was quantified with strongly varying concentrations from 7th to 9th May 2017. The averaged concentration in this period was 65.2 ng m^{-3}. At the same time, oxalate was measured with an averaged concentration of 97.4 ng m^{-3} agreeing with impactor measurements of van Pinxteren et al. (2014) and references therein. The diurnal cycle of oxalate in Fig. 9b shows the same pattern as formic acid, indicating a photochemical formation.

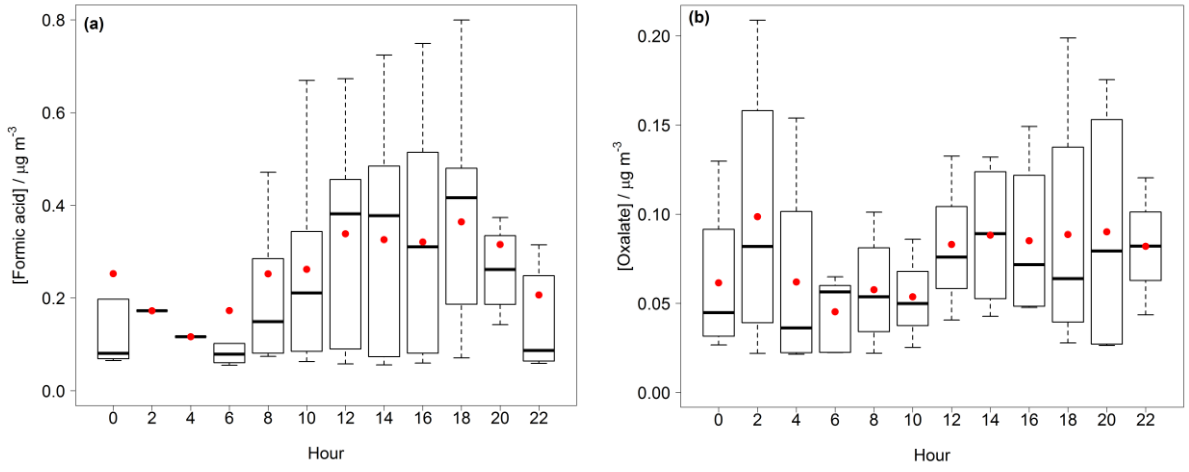

Figure 9. Box-Whisker-Plot for the diurnal variation of gaseous formic acid (a) and particulate oxalate (b) in Melpitz for the example application in the field. The red dots represent the mean, the box the 25th and 75th percentile and the upper whisker the 75th percentile plus the 1.5-fold interquartile range (IQR) and the lower whisker the 25th percentile minus the 1.5-fold IQR.

Methanesulfonate ranged between LOD and approximately 100 ng m^{-3}, while a peak of 465 ng m^{-3} was detected on 8th May 2017. This happened simultaneously with a sudden increase of wind speed. Northeasterly winds transporting marine air masses to Melpitz appear to be the most likely explanation for this (Hoffmann et al., 2016;Lana et al., 2011). These examples demonstrate the successful recording of time-resolved organic acid concentrations in both gas and particle-phase. Further in-depth analyses and detailed results of the one-year measurements with the extended MARGA system will be presented elsewhere (Stieger et al., manuscript in preparation).

4 Conclusions

An extension of the MARGA analysis was described to quantify online low-molecular weight organic acids. Therefore, the MARGA was combined with a new setup consisting of an autosampler and a Compact-IC with internal pre-concentration. Laboratory optimizations of the Compact-IC were performed to improve the separation of the target organic acids formate, acetate, propionate, butyrate, glycolate, pyruvate, oxalate, malonate, succinate, malate, glutarate, and methanesulfonate. An upgrade to a gradient system and an extension of the Metrosep A Supp 16 column to a total length of 400 mm allowed for a satisfactory separation of all MCAs and DCAs with low limits of detection and precisions.

The example application of the system in May 2017 illustrated high concentrations of formic acid and oxalate in the late afternoon, indicating a photochemical formation by atmospheric precursors. Variations of the wind direction resulted in sudden changes in the concentrations, as it was the case for methanesulfonate.

The results of the example application proved the suitability of the MARGA extension for field measurements. Compared to other online systems, the variety of quantifiable organic acids in the gas and particle-phase is unique. The application of this online method reduces laboratory work and sampling artifacts by filter and impactor measurements. Additionally, the time resolution of two hours allowed the investigation of diurnal cycles, improving the knowledge of their primary and/or secondary sources. For the investigation of tropospheric multiphase chemistry, simultaneous quantification of the gas and the particle-phase concentrations promises interesting analyses of the phase distribution of each organic acid.

Data availability

Data can be made available from authors on request.

Author contribution

HH concepted the MARGA extension. BS performed the experimental development, the calculations, the combination in the field, the measurements and wrote the manuscript. GS, DvP and HH contributed ideas and suggestions during the method development and the field measurements. AG helped during infrastructural issues in Melpitz. All authors provided additional input and comments during the preparation of the manuscript.

Competing interests

The authors declare that they have no conflict of interest.

Acknowledgements

We thank R. Rabe for the support, especially in the field. The authors acknowledge financial support of this study and deployment of the MARGA system by the German Federal Environment Agency (UBA) research foundation under contract No 52436 as well as from the European Regional Development fund by the European Union under contract No 100188826. This study is partly supported by ACTRIS-2 (Aerosol, Clouds, and Trace gases Research InfraStructure network) from the European Union's Horizon 2020 research and innovation programme under grant agreement No 654109.

References

Bao, L. F., Matsumoto, M., Kubota, T., Sekiguchi, K., Wang, Q. Y., and Sakamoto, K.: Gas/particle partitioning of low-molecular-weight dicarboxylic acids at a suburban site in Saitama, Japan, Atmos Environ, 47, 546-553, 10.1016/j.atmosenv.2009.09.014, 2012.

Bock, N., Baum, M. M., Anderson, M. B., Pesta, A., and Northrop, W. F.: Dicarboxylic Acid Emissions from Aftertreatment Equipped Diesel Engines, Environ Sci Technol, 51, 13036-13043, 10.1021/acs.est.7b03868, 2017.

Boreddy, S. K. R., Mochizuki, T., Kawamura, K., Bikkina, S., and Sarin, M. M.: Homologous series of low molecular weight (C-1-C-10) monocarboxylic acids, benzoic acid and hydroxyacids in fine-mode (PM2.5) aerosols over the Bay of Bengal: Influence of heterogeneity in air masses and formation pathways, Atmos Environ, 167, 170-180, 10.1016/j.atmosenv.2017.08.008, 2017.

Boring, C. B., Al-Horr, R., Genfa, Z., Dasgupta, P. K., Martin, M. W., and Smith, W. F.: Field measurement of acid gases and soluble anions in atmospheric particulate matter using a parallel plate wet denuder and an alternating filter-based automated analysis system, Anal Chem, 74, 1256-1268, 10.1021/ac015643r, 2002.

Chen, X., Walker, J. T., and Geron, C.: Chromatography related performance of the Monitor for AeRosols and GAses in ambient air (MARGA): laboratory and field-based evaluation, Atmos Meas Tech, 10, 3893-3908, 10.5194/amt-10-3893-2017, 2017.

Crisp, T. A., Brady, J. M., Cappa, C. D., Collier, S., Forestieri, S. D., Kleeman, M. J., Kuwayama, T., Lerner, B. M., Williams, E. J., Zhang, Q., and Bertram, T. H.: On the primary emission of formic acid from light duty gasoline vehicles and ocean-going vessels, Atmos Environ, 98, 426-433, 10.1016/j.atmosenv.2014.08.070, 2014.

Dawson, G. A., Farmer, J. C., and Moyers, J. L.: Formic and Acetic-Acids in the Atmosphere of the Southwest USA, Geophys Res Lett, 7, 725-728, 10.1029/GL007i009p00725, 1980.

DIN 32645: Chemische Analytik - Nachweis-, Erfassungs- und Bestimmungsgrenze unter Wiederholbedingungen - Begriffe, Verfahren, Auswertung, 2008.

DIN ISO 8466-2: Wasserbeschaffenheit - Kalibrierung und Auswertung analytischer Verfahren und Beurteilung von Verfahrenskenndaten - Teil 2: Kalibrierstrategie für nichtlineare Kalibrierfunktionen zweiten Grades, 2004.

Falkovich, A. H., Graber, E. R., Schkolnik, G., Rudich, Y., Maenhaut, W., and Artaxo, P.: Low molecular weight organic acids in aerosol particles from Rondonia, Brazil, during the biomass-burning, transition and wet periods, Atmos Chem Phys, 5, 781-797, 10.5194/acp-5-781-2005, 2005.

Fisseha, R., Dommen, J., Gaeggeler, K., Weingartner, E., Samburova, V., Kalberer, M., and Baltensperger, U.: Online gas and aerosol measurement of water soluble carboxylic acids in Zurich, J Geophys Res-Atmos, 111, 10.1029/2005jd006782, 2006.

Friedman, B., Link, M. F., Fulgham, S. R., Brophy, P., Galang, A., Brune, W. H., Jathar, S. H., and Farmer, D. K.: Primary and Secondary Sources of Gas-Phase Organic Acids from Diesel Exhaust, Environ Sci Technol, 51, 10872-10880, 10.1021/acs.est.7b01169, 2017.

Funk, W., Dammann, V., and Donnevert, G.: Qualitätssicherung in der Analytischen Chemie, WILEY-VCH Verlag, Weinheim, 2005.

Granby, K., Egeløv, A. H., Nielsen, T., and Lohse, C.: Carboxylic acids: Seasonal variation and relation to chemical and meteorological parameters, J Atmos Chem, 28, 195-207, 10.1023/A:1005877419395, 1997.

Himanen, M., Prochazka, P., Hänninen, K., and Oikari, A.: Phytotoxicity of low-weight carboxylic acids, Chemosphere, 88, 426-431, 10.1016/j.chemosphere.2012.02.058, 2012.

Hoffmann, E. H., Tilgner, A., Schrödner, R., Bräuer, P., Wolke, R., and Herrmann, H.: An advanced modeling study on the impacts and atmospheric implications of multiphase dimethyl sulfide chemistry, P Natl Acad Sci USA, 113, 11776-11781, 10.1073/pnas.1606320113, 2016.

Howard, P. M., and Meylan, W. M.: Handbook of Physical Properties of Organic Chemicals, CRC Press, Boca Raton, 1997.

Jones, B. T., Muller, J. B. A., O'Shea, S. J., Bacak, A., Le Breton, M., Bannan, T. J., Leather, K. E., Booth, A. M., Illingworth, S., Bower, K., Gallagher, M. W., Allen, G., Shallcross, D. E., Bauguitte, S. J. B., Pyle, J. A., and Percival, C. J.: Airborne measurements of HC(O)OH in the European Arctic: A winter - summer comparison, Atmos Environ, 99, 556-567, 10.1016/j.atmosenv.2014.10.030, 2014.

Kawamura, K., and Kaplan, I. R.: Motor Exhaust Emissions as a Primary Source for Dicarboxylic Acids in Los Angeles Ambient Air, Environ Sci Technol, 21, 105-110, 10.1021/es00155a014, 1987.

Kawamura, K., Ono, K., Tachibana, E., Charriere, B., and Sempere, R.: Distributions of low molecular weight dicarboxylic acids, ketoacids and α-dicarbonyls in the marine aerosols collected over the Arctic Ocean during late summer, Biogeosciences, 9, 4725-4737, 10.5194/bg-9-4725-2012, 2012.

Kawamura, K., and Bikkina, S.: A review of dicarboxylic acids and related compounds in atmospheric aerosols: Molecular distributions, sources and transformation, Atmospheric Research, 170, 140-160, 10.1016/j.atmosres.2015.11.018, 2016.

Khare, P., Satsangi, G. S., Kumar, N., Kumari, K. M., and Srivastava, S. S.: Surface measurements of formaldehyde and formic and acetic acids at a subtropical semiarid site in India, J Geophys Res-Atmos, 102, 18997-19005, 10.1029/97jd00735, 1997.

Ku, Y. P., Yang, C., Lin, G. Y., and Tsai, C. J.: An Online Parallel-Plate Wet Denuder System for Monitoring Acetic Acid Gas, Aerosol Air Qual Res, 10, 479-488, 10.4209/aaqr.2010.03.0023, 2010.

Kuo, S. C., Tsai, Y. I., Tsai, C. H., and Hsieh, L. Y.: Carboxylic acids in PM2.5 over Pinus morrisonicola forest and related photoreaction mechanisms identified via Raman spectroscopy, Atmos Environ, 45, 6741-6750, 10.1016/j.atmosenv.2011.08.007, 2011.

Lana, A., Bell, T. G., Simo, R., Vallina, S. M., Ballabrera-Poy, J., Kettle, A. J., Dachs, J., Bopp, L., Saltzman, E. S., Stefels, J., Johnson, J. E., and Liss, P. S.: An updated climatology of surface dimethlysulfide concentrations and emission fluxes in the global ocean, Global Biogeochem Cy, 25, 10.1029/2010gb003850, 2011.

Lee, B., Hwangbo, Y., and Lee, D. S.: Determination of Low Molecular Weight Monocarboxylic Acid Cases in the Atmosphere by Parallel Plate Diffusion Scrubber-Ion Chromatography, J Chromatogr Sci, 47, 516-522, 10.1093/chromsci/47.7.516, 2009.

Legrand, M., Preunkert, S., Oliveira, T., Pio, C. A., Hammer, S., Gelencser, A., Kasper-Giebl, A., and Laj, P.: Origin of C_2-C_5 dicarboxylic acids in the European atmosphere inferred from year-round aerosol study conducted at a west-east transect, J Geophys Res-Atmos, 112, 10.1029/2006jd008019, 2007.

Lim, H. J., Carlton, A. G., and Turpin, B. J.: Isoprene forms secondary organic aerosol through cloud processing: Model simulations, Environ Sci Technol, 39, 4441-4446, 10.1021/es048039h, 2005.

Limbeck, A., Kraxner, Y., and Puxbaum, H.: Gas to particle distribution of low molecular weight dicarboxylic acids at two different sites in central Europe (Austria), J Aerosol Sci, 36, 991-1005, 10.1016/j.jaerosci.2004.11.013, 2005.

Liu, J. M., Zhang, X. L., Parker, E. T., Veres, P. R., Roberts, J. M., de Gouw, J. A., Hayes, P. L., Jimenez, J. L., Murphy, J. G., Ellis, R. A., Huey, L. G., and Weber, R. J.: On the gas-particle partitioning of soluble organic aerosol in two urban atmospheres with contrasting emissions: 2. Gas and particle phase formic acid, J Geophys Res-Atmos, 117, 10.1029/2012jd017912, 2012.

Millet, D. B., Baasandorj, M., Farmer, D. K., Thornton, J. A., Baumann, K., Brophy, P., Chaliyakunnel, S., de Gouw, J. A., Graus, M., Hu, L., Koss, A., Lee, B. H., Lopez-Hilfiker, F. D., Neuman, J. A., Paulot, F., Peischl, J., Pollack, I. B., Ryerson, T. B., Warneke, C., Williams, B. J., and Xu, J.: A large and ubiquitous source of atmospheric formic acid, Atmos Chem Phys, 15, 6283-6304, 10.5194/acp-15-6283-2015, 2015.

Miyazaki, Y., Sawano, M., and Kawamura, K.: Low-molecular-weight hydroxyacids in marine atmospheric aerosol: evidence of a marine microbial origin, Biogeosciences, 11, 4407-4414, 10.5194/bg-11-4407-2014, 2014.

Mochizuki, T., Kawamura, K., Miyazaki, Y., and Boreddy, S. K. R.: Distributions and sources of gaseous and particulate low molecular weight monocarboxylic acids in a deciduous broadleaf forest from northern Japan, Atmospheric Chemistry and Physics Discussions, 2018.

Müller, K., van Pinxteren, D., Plewka, A., Svrcina, B., Kramberger, H., Hofmann, D., Bächmann, K., and Herrmann, H.: Aerosol characterisation at the FEBUKO upwind station Goldlauter (II): Detailed organic chemical characterisation, Atmos Environ, 39, 4219-4231, 10.1016/j.atmosenv.2005.02.008, 2005.

Nah, T., Ji, Y., Tanner, D. J., Guo, H. Y., Sullivan, A. P., Ng, N. L., Weber, R. J., and Huey, L. G.: Real-time measurements of gas-phase organic acids using SF_6^- chemical ionization mass spectrometry, Atmos Meas Tech, 11, 5087-5104, 10.5194/amt-11-5087-2018, 2018.

Pommier, M., Clerbaux, C., Coheur, P. F., Mahieu, E., Müller, J. F., Paton-Walsh, C., Stavrakou, T., and Vigouroux, C.: HCOOH distributions from IASI for 2008-2014: comparison with ground-based FTIR measurements and a global chemistry-transport model, Atmos Chem Phys, 16, 8963-8981, 10.5194/acp-16-8963-2016, 2016.

Preunkert, S., Legrand, M., Jourdain, B., and Dombrowski-Etchevers, I.: Acidic gases (HCOOH, CH_3COOH, HNO_3, HCl, and SO_2) and related aerosol species at a high mountain Alpine site (4360 m elevation) in Europe, J Geophys Res-Atmos, 112, 10.1029/2006jd008225, 2007.

Röhrl, A., and Lammel, G.: Determination of malic acid and other C-4 dicarboxylic acids in atmospheric aerosol samples, Chemosphere, 46, 1195-1199, 10.1016/S0045-6535(01)00243-0, 2002.

Rumsey, I. C., and Walker, J. T.: Application of an online ion-chromatography-based instrument for gradient flux measurements of speciated nitrogen and sulfur, Atmos Meas Tech, 9, 2581-2592, 10.5194/amt-9-2581-2016, 2016.

Sabbioni, C., Ghedini, N., and Bonazza, A.: Organic anions in damage layers on monuments and buildings, Atmos Environ, 37, 1261-1269, 10.1016/S1352-2310(02)01025-7, 2003.

Schöne, L., and Herrmann, H.: Kinetic measurements of the reactivity of hydrogen peroxide and ozone towards small atmospherically relevant aldehydes, ketones and organic acids in aqueous solutions, Atmos Chem Phys, 14, 4503-4514, 10.5194/acp-14-4503-2014, 2014.

Schultz Tokos, J. J., Tanaka, S., Morikami, T., Shigetani, H., and Hashimoto, Y.: Gaseous Formic and Acetic-Acids in the Atmosphere of Yokohama, Japan, J Atmos Chem, 14, 85-94, 10.1007/Bf00115225, 1992.

Spindler, G., Hesper, J., Brüggemann, E., Dubois, R., Müller, T., and Herrmann, H.: Wet annular denuder measurements of nitrous acid: laboratory study of the artefact reaction of NO_2 with S(IV) in aqueous solution and comparison with field measurements, Atmos Environ, 37, 2643-2662, 10.1016/S1352-2310(03)00209-7, 2003.

Spindler, G., Müller, K., Brüggemann, E., Gnauk, T., and Herrmann, H.: Long-term size-segregated characterization of PM_{10}, $PM_{2.5}$, and PM_1 at the IfT research station Melpitz downwind of Leipzig (Germany) using high and low-volume filter samplers, Atmos Environ, 38, 5333-5347, 10.1016/j.atmosenv.2003.12.047, 2004.

Spindler, G., Grüner, A., Müller, K., Schlimper, S., and Herrmann, H.: Long-term size-segregated particle (PM_{10}, $PM_{2.5}$, PM_1) characterization study at Melpitz - influence of air mass inflow, weather conditions and season, J Atmos Chem, 70, 165-195, 10.1007/s10874-013-9263-8, 2013.

Stavrakou, T., Muller, J. F., Peeters, J., Razavi, A., Clarisse, L., Clerbaux, C., Coheur, P. F., Hurtmans, D., De Maziere, M., Vigouroux, C., Deutscher, N. M., Griffith, D. W. T., Jones, N., and Paton-Walsh, C.: Satellite evidence for a large source of formic acid from boreal and tropical forests, Nat Geosci, 5, 26-30, 10.1038/Ngeo1354, 2012.

Stieger, B., Spindler, G., Fahlbusch, B., Müller, K., Grüner, A., Poulain, L., Thöni, L., Seitler, E., Wallasch, M., and Herrmann, H.: Measurements of PM_{10} ions and trace gases with the online system MARGA at the research station Melpitz in Germany - A five-year study, J Atmos Chem, 75, 33-70, 10.1007/s10874-017-9361-0, 2018.

Sun, X., Wang, Y., Li, H. Y., Yang, X. Q., Sun, L., Wang, X. F., Wang, T., and Wang, W. X.: Organic acids in cloud water and rainwater at a mountain site in acid rain areas of South China, Environ Sci Pollut R, 23, 9529-9539, 10.1007/s11356-016-6038-1, 2016.

Tilgner, A., and Herrmann, H.: Radical-driven carbonyl-to-acid conversion and acid degradation in tropospheric aqueous systems studied by CAPRAM, Atmos Environ, 44, 5415-5422, 10.1016/j.atmosenv.2010.07.050, 2010.

van Pinxteren, D., Plewka, A., Hofmann, D., Müller, K., Kramberger, H., Svrcina, B., Bachmann, K., Jaeschke, W., Mertes, S., Collett, J. L., and Herrmann, H.: Schmücke hill cap cloud and valley stations aerosol characterisation during FEBUKO (II): Organic compounds, Atmos Environ, 39, 4305-4320, 10.1016/j.atmosenv.2005.02.014, 2005.

van Pinxteren, D., Brüggemann, E., Gnauk, T., Iinuma, Y., Müller, K., Nowak, A., Achtert, P., Wiedensohler, A., and Herrmann, H.: Size- and time-resolved chemical particle characterization during CAREBeijing-2006: Different pollution regimes and diurnal profiles, J Geophys Res-Atmos, 114, 10.1029/2008jd010890, 2009.

van Pinxteren, D., Neusüß, C., and Herrmann, H.: On the abundance and source contributions of dicarboxylic acids in size-resolved aerosol particles at continental sites in central Europe, Atmos Chem Phys, 14, 3913-3928, 10.5194/acp-14-3913-2014, 2014.

van Pinxteren, D., Fomba, K. W., Mertes, S., Müller, K., Spindler, G., Schneider, J., Lee, T., Collett, J. L., and Herrmann, H.: Cloud water composition during HCCT-2010: Scavenging efficiencies, solute concentrations, and droplet size dependence of inorganic ions and dissolved organic carbon, Atmos Chem Phys, 16, 3185-3205, 10.5194/acp-16-3185-2016, 2016.

Veres, P. R., Roberts, J. M., Cochran, A. K., Gilman, J. B., Kuster, W. C., Holloway, J. S., Graus, M., Flynn, J., Lefer, B., Warneke, C., and de Gouw, J.: Evidence of rapid production of organic acids in an urban air mass, Geophys Res Lett, 38, 10.1029/2011gl048420, 2011.

Zander, R., Duchatelet, P., Mahieu, E., Demoulin, P., Roland, G., Servais, C., Auwera, J. V., Perrin, A., Rinsland, C. P., and Crutzen, P. J.: Formic acid above the Jungfraujoch during 1985-2007: observed variability, seasonality, but no long-term background evolution, Atmos Chem Phys, 10, 10047-10065, 10.5194/acp-10-10047-2010, 2010.

Zhou, Y., Huang, X. H., Bian, Q. J., Griffith, S. M., Louie, P. K. K., and Yu, J. Z.: Sources and atmospheric processes impacting oxalate at a suburban coastal site in Hong Kong: Insights inferred from 1year hourly measurements, J Geophys Res-Atmos, 120, 9772-9788, 10.1002/2015jd023531, 2015.